Terrain-Based Simulation of IEEE 802.11a and b Physical Layers on the Martian Surface

Anirudh Daga, Gaylon R. Lovelace, Deva K. Borah, *Member, IEEE,* and Phillip L. De Leon, *Senior Member, IEEE*

Abstract

This paper presents results concerning the use of IEEE 802.11a and b wireless local area network (WLAN) standards for proximity wireless networks on the Martian surface. The radio frequency (RF) environment on the Martian surface is modeled using high-resolution digital elevation maps (DEMs) of Gusev Crater and Meridiani Planum (Hematite) as sample sites. The resulting propagation path loss models are then used in a physical layer (PHY) simulation. Our results show that Martian terrain as represented by the sites studied, can create multipath conditions which in turn affect 802.11a and b PHY performance. However, with a few tens of milliwatts of radiated power and antenna heights within 1–2 m, orthogonal frequency division multiplexing (OFDM)-based 802.11a can have very good PHY performance in terms of bit- and packet-error rates for distances up to a few hundred meters; 802.11b, which is based on direct-sequence spread spectrum (DSSS), is found to be much more adversely affected in the multipath environment. The DEM-based simulation methodology presented here may be more useful to mission planners than generic statistical models.

Index Terms

Wireless LAN, Communication system performance.

I. Introduction

NASA'S long-term goals for the exploration of Mars include the use of rovers and sensors which intercommunicate through proximity wireless networks. These networks are designed to have a short range, relatively low cost, and short lifespan and are obviously required to be reliable, robust, and power efficient. Of considerable interest is the applicability of wireless local area network (WLAN) standards such as IEEE 802.11a, b, and g for such planetary surface networks. However, since these standards were primarily developed for indoor use, there are many factors in the outdoor environment that can limit network performance and thus need to be studied before consideration for application in a planetary exploration mission. In particular, lack of man-made structures and vegetation, a negligible atmosphere, and the presence of unique terrain features on the Martain surface raise questions about the exact behavior of WLAN technology on that planet. A methodology to address questions such as how much transmission power is needed for a reliable link, how the distance affects receiver's performance, and the effect of antenna heights on communications can provide valuable guidelines for future mission planners.

Numerous publications have considered many of the steps toward such a study of WLAN performance in an outdoor environment, albeit for Earth. These steps include channel modeling and performance analysis of the physical layer (PHY) in the multipath environment. With respect to channel modeling at the 2.4 and 5 GHz WLAN frequencies, most studies have focused either on the indoor office environment or outdoor urban environment [1], [2], [3]. In [1], the authors considered IEEE 802.11a and g and simulated path loss, coverage, and medium access control (MAC) throughput in a corporate office environment using detailed models of the building and ray-tracing methods to carefully simulate the indoor multipath propagation. It is well known that such methods which take into account detailed models of the propagation environment provide more accurate channel models than other simple statistical models. Their work demonstrates the utility of using environment-based radio frequency (RF) modeling in order to evaluate PHY and MAC performance but is limited to the indoor environment. In [2], the authors develop empirical channel models for the outdoor urban environment based on measured data. They demonstrate that in the outdoor urban environment, large man-made objects are a major source of long multipaths and significant rms delay spreads and take this in account when developing their channel models.

With respect to performance analysis of the PHY in an outdoor multipath environment, several studies have focussed on the application of WLAN standards for cellular telephony. In [4], the authors examined the use of 802.11b (1 Mbps) for an outdoor cellular network and in particular, investigated the impact of multipath on bit error rate (BER) performance by assuming a simple multipath channel model with rms delay spreads of 250 ns, 1 μs, and 3 μs. Their work demonstrates that higher delay spreads associated with the outdoor environment led to poorer 802.11b PHY performance. In [5], the authors tested 802.11a outdoors in a city environment and measured network throughput as a function of user mobility.

This work was presented in part at the 2005 and 2006 IEEE Aerospace Conference, Big Sky, MT. This work was supported by NASA Grant NAG3-2864.

A. Daga is with Motorola. D. K. Borah, P. L. De Leon, and G. R. Lovelace, are with the Klipsch School of Electrical and Computer Engineering, New Mexico State University, Las Cruces, NM 88003 USA.

* Direct all correspondence regarding this manuscript to Dr. Phillip De Leon (pdeleon@nmsu.edu).

Despite these studies, there are several reasons for examining WLAN performance exclusively for the Martian surface. First, most studies have only considered the urban environment which does not represent the Martian surface where terrain features, rather than man-made structures, play the dominant role. In fact, many of these studies take into account atmospheric effects which are largely non-existent on Mars. Second, although these studies can provide qualitative interpretations that may be generally applicable to the Martian environment, direct extrapolation of results based on generic multipath models may not lead to accurate results in the Martian environment where terrain is a key factor. Third, although application of WLAN technologies to the outdoor environment can likely take advantage of elevated antenna heights for better coverage, there are clear limitations on antenna heights in robotic space missions.

In this paper, we investigate PHY performance of the 802.11a and b WLAN standards under a carefully simulated Martian RF environment. These two standards were chosen due to their early and widespread adoption, large body of existing research, and availability of tools for such an investigation. We begin by simulating the multipaths which arise from topographic features on the Martian surface at the 2.4 and 5.25 GHz center frequencies of 802.11b and a, respectively. These multipaths are collectively described by a power delay profile (PDP) between transmitter and receiver i.e. received power in each multipath component arriving at a particular time delay. To compute PDPs, we utilize a commercial RF propagation modeling software (with appropriate modifications for the Martian environment) which uses 10.4 m/pixel digital elevation maps (DEMs) of the Gusev Crater and the Meridiani Planum (Hematite) regions on Mars. The software allows user-specified communication system parameters (antenna heights, radiated power, etc.) and environmental parameters. Terrain-based, propagation modeling based on high-resolution DEMs is fairly common with network planners in the cellular telephone industry but to our knowledge, has not been used by mission planners for communications design in planetary or lunar surface applications.

Next, using PDP data we simulate PHY performance of the WLAN standards at various Martian sites. We study BERs and packet error rates (PERs) as a function of the distance between transmitter and receiver, SNR, antenna height, radiated power, and data rate mode for the two WLAN standards. Different data rates in the standards are achieved by varying the modulation type and/or the channel coding rates and can perform very differently depending on the environment [1]. As we will show, the multipaths which arise from the Martian terrain can severely affect PHY performance of 802.11b and to a lesser extent 802.11a. The Orthogonal Frequency Division Multiplexing (OFDM)-based 802.11a can tolerate strong multipaths provided the excess delay spread does not exceed the 0.8 μs cyclic prefix duration; in the event this is not true (as seen in a few links we simulated), the performance drops off rapidly. For Direct-Sequence Spread Spectrum (DSSS)-based 802.11b, using a RAKE receiver significantly improves performance in a strong multipath environment.

This paper is organized as follows. In Section II, we provide details and results from the first part of the study on simulation of the multipath environment on Mars. In Section III, we describe the simulation methodology and present results from the second part of the study regarding PHY performance in the simulated Martian environment and in Section IV, we conclude the article.

II. Modeling the Martian RF Environment

One of the main issues with wireless communications channels is the time dispersion due to multipath propagation. The time dispersion is often described with a PDP, $P(\tau)$ obtained by averaging, over a local area at various time instants, the squared channel impulse response between transmitter and receiver [6]

$$P(\tau) \approx \overline{g|h_b(t;\tau)|^2} \tag{1}$$

where g is the total transmitter-to-receiver power gain and $h_b(t;\tau)$ is the time-varying channel impulse response. In our case, since the transmitter, receiver, and reflectors are all fixed, averaging over the time instants has no significance for PDPs. In order to compute PDPs for various transmit/receive configurations on the Martian surface, we have utilized a commercial RF propagation modeling software package from ATDI called *ICS telecom* [7]. This package employs proprietary techniques based on ray-tracing, and is widely used in the cellular telecommunications industry. With proper modifications (described below) and high-resolution DEMs, we are able to compute PDPs out to several microseconds with a temporal resolution of 10 ns [8].

A. Selection of DEMs and Sites

High-resolution DEMs (approximately 10.4 m/pixel) of the Gusev Crater and Hematite regions were developed by the United States Geological Survey (USGS) to assist in planning the 2004 Mars Exploration Rover (MER) mission [9], [10]. For this study, the Gusev1, Hematite4, and Hematite5 DEMs were selected for their variety of topographic features [11]. The specific transmitter locations used in simulations were chosen to sample the local topography and are given in Table I.

B. Propagation Model

In order to compute PDPs, we selected the Irregular Terrain Model (ITM) as the propagation model [12]. Several Mars-specific modifications to the ITM were made. These include electrical ground constants (permittivity, conductivity estimated as 4 F/m, 10^{-8} S/m respectively) and negligible atmospheric attenuation and refraction [13], [14], [15]. Other parameters within the ITM are chosen based on the WLAN standards or on other known data regarding the Martian environment [8].

TABLE I
SITE LOCATIONS FOR TRANSMITTER.

Site	*Mars Latitude*	*Mars Longitude*	*Elevation*
Gusev1 Site1	$14^\circ\ 47'\ 39.35''$ S	$176^\circ\ 1'\ 29.18''$ E	83 m
Gusev1 Site2	$14^\circ\ 58'\ 41.95''$ S	$176^\circ\ 2'\ 53.51''$ E	158 m
Gusev1 Site3	$15^\circ\ 11'\ 35.66''$ S	$176^\circ\ 4'\ 31.23''$ E	24 m
Hematite4	$2^\circ\ 11'\ 0.69''$ S	$-5^\circ\ 53'\ 5.16''$ E	66 m
Hematite5	$1^\circ\ 52'\ 29.16''$ S	$-5^\circ\ 25'\ 39.59''$ E	32 m

C. Multipath Simulation Results

PDPs were computed for a transmitter located at the coordinates specified in Table I and a receiver at various distances to the south; antenna mast heights (all antennae are assumed isotropic) were also varied. PDPs were computed using 1 W total transmitted power and scaled linearly for other power levels. Tables II and III provide rms delay spread and received power data for the combination of 1.5 m antenna heights and 1 W radiated power at various distances between transmitter and receiver positioned to the south. It is interesting to note from the data that due to favorable terrain conditions, there are some cases where the rms delay spread is smaller and the received power is greater even though the distances are greater (see for example Gusev1 Site1 20 m and 200 m). Such favorable conditions can arise for example, when a receiver is located on an upward slope with Fresnel zone clearance. By carefully factoring in terrain, transmission power savings may be realized with an appropriate rover path plan. The delay spreads in Table II are largely on the same order as those assumed by other investigators [4]. However, rather than assuming a generic multipath profile, we have derived the characteristic multipath response for each transmitter and receiver location pair. This extends applicability to situations such as planetary missions, where it is not possible to empirically validate any parameterized statistical model. It also enables analysis of exceptional cases, where the statistical model would become invalid.

TABLE II
RMS DELAY SPREAD (μS) VS. DISTANCE BETWEEN TRANSMITTER/RECEIVER (1.5 M ANTENNA HEIGHT; 1 W RADIATED POWER).

Dist (m)	Gusev1 Site1		Gusev1 Site2		Gusev1 Site3		Hematite4		Hematite5	
	2.4 GHz	5 GHz	2.4 GHz	5 GHz	2.4 GHz	5 GHz	2.4 GHz	5 GHz	2.4 GHz	5 GHz
20	0.268	0.266	0.186	0.193	0.170	0.181	0.634	0.623	0.913	0.791
50	0.203	0.201	0.156	0.164	0.101	0.081	0.625	0.613	0.694	0.604
100	0.155	0.154	0.126	0.133	0.065	0.067	0.564	0.518	0.498	0.421
200	0.153	0.127	0.719	0.722	0.089	0.095	0.297	0.255	0.229	0.155
500	0.092	0.074	0.477	0.468	9.210	7.094	0.088	0.066	0.204	0.155
1000	1.864	17.855	N/A	N/A	0.718	0.766	0.685	0.668	0.316	0.287

TABLE III
RECEIVED POWER (NW) VS. DISTANCE BETWEEN TRANSMITTER/RECEIVER (1.5 M ANTENNA HEIGHT; 1 W RADIATED POWER).

Dist (m)	Gusev1 Site1		Gusev1 Site2		Gusev1 Site3		Hematite4		Hematite5	
	2.4 GHz	5 GHz	2.4 GHz	5 GHz	2.4 GHz	5 GHz	2.4 GHz	5 GHz	2.4 GHz	5 GHz
20	79.3	40.9	78.6	38.3	118.8	52.0	114.3	59.2	88.6	45.9
50	75.1	38.6	56.5	26.7	101.9	45.2	94.1	49.1	69.1	36.2
100	71.4	36.4	54.6	25.8	103.2	45.9	80.7	47.0	56.0	29.2
200	206.0	70.0	0.2	0.1	80.7	34.8	46.1	29.3	55.3	28.6
500	145.0	61.7	0.02	0.01	0.0001	1e$-$5	43.3	22.5	89.0	42.3
1000	0.001	0.0001	N/A	N/A	3e$-$5	1e$-$6	0.2	0.04	2e$-$6	2e$-$7

III. PHYSICAL LAYER PERFORMANCE IN THE MARTIAN ENVIRONMENT

In this section, we describe the simulation methodology, performance metrics and results of 802.11a and b PHY performance in the simulated Martian environment. Unless otherwise noted, the transmitter is located at the coordinates in Table I, the receiver is located 100 m to the south of the transmitter, and data rate modes are 12, 11 Mbps for 802.11a, b respectively for fair performance comparisons. BER values represent results after the channel decoder when a channel code is used.

A. Physical Layer Simulation

The different transmission rates of IEEE 802.11a PHY are simulated by varying the modulation type and/or the channel coding rates as specified in the standard [16]. The system uses 52 subcarriers that are modulated using BPSK, QPSK, 16- or 64- quadrature amplitude modulation (QAM). The PHY protocol data unit (PPDU) consists of three parts: (1) a 12 symbol PHY convergence procedure (PLCP) preamble, (2) one OFDM SIGNAL symbol, and (3) OFDM data symbols. The data to be transmitted are scrambled to remove spectral lines from the data, are then convolutionally encoded with a rate 1/2 encoder,

and puncturing is performed if necessary. All encoded data bits are interleaved using two steps. First, consecutive coded bits are mapped to non-adjacent subcarriers. The second step maps consecutive coded bits onto the less and more significant bits of the constellation. The OFDM symbols are transmitted using a relatively long cyclic prefix of duration $T_{\mathrm{GI}} = T_{\mathrm{FFT}}/4$, where T_{FFT} is the duration of an OFDM symbol without the cyclic prefix and is equal to 3.2 μs. Thus the symbol interval including the cyclic prefix is 4.0 μs, PLCP preamble duration is 16 μs, and the SIGNAL symbol lasts 4.0 μs.

The IEEE 802.11b DSSS can provide data rates of 1, 2, 5.5 and 11 Mbit/s. The basic data rate of 1 Mbit/s is provided using differential binary phase shift keying (DBPSK) while the 2 Mbit/s rate uses differential quadrature phase shift keying (DQPSK). The above two data rates employ 11 chip long Barker sequences for spreading with a chip rate of 11 MHz. Higher data rates of 5.5 Mbit/s and 11 Mbit/s use complementary code keying (CCK) at the same chipping rate of 11 Mchips/s. The PPDU format for IEEE 802.11b also consists of three parts: (1) a PLCP preamble, (2) a PLCP header, and (3) PSDU. The header consists of signal, service, length and cyclic redundancy code (CRC) fields. The long PLCP preamble and header are both transmitted using 1 Mbit/s DBPSK modulation. In the case of a short PLCP, the preamble is transmitted using 1 Mbit/s while the header is transmitted using 2 Mbit/s. The transmitted data bits are scrambled at the transmitter and descrambled at the receiver.

In our study, IEEE 802.11a and b PPDUs are generated as specified in the standards. In order to evaluate PHY performance on the Martian environment, an impulse response obtained from the PDP must be convolved with the data waveform. As defined in (1), however, a PDP is a power profile and thus has no phase information. In order to generate a complex baseband impulse response, we multiply the channel coefficient magnitudes (square root of the PDP) with complex Gaussian random numbers, which also allows us to obtain an average overall effect over an ensemble. This ensemble represents uncertain factors, including magnitude and phase variations of the individual paths, over an area caused by the uncertainty in the receiver's exact location due to the limited resolution of the DEMs. For 802.11b simulations, the resulting impulse response is fractionally resampled in order to match the sample time of the oversampled (square root raised cosine filtered) data. With this processing, the complex baseband transmit signal is then convolved with the impulse response and white Gaussian noise is added to achieve either a specified E_b/N_0 or to match receiver noise estimates given in [17]. The resulting output signal is then processed by the receiver. For both 802.11a and b, only truncated channel impulse responses are estimated at the receiver using the corresponding PLCP preamble. Unless otherwise noted, the 802.11b receiver estimates approximately 100 multipath coefficients using least squares and uses the estimated coefficients for RAKE reception. The packet size was chosen to be 1024 data bits. While the 802.11 standard allows much larger packets, we assume that the most important concern in a planetary exploration environment would be control and telemetry data, which would likely point to smaller data packets. Furthermore, since we simulate a quasi-static channel (the multipath response is constant within a packet, and the complex phase/fading vector is independent for each packet), simulating a larger number of smaller packets provides more significant statistics in limited computation time. Up to 20,000 packets were simulated for the various cases and each simulation was halted early if it reached 2000 packet errors. BER simulation results for both WLAN standards in the AWGN channel agreed very closely with the results presented in [18], [19].

We consider BER and PER performance and these are estimated separately by simulating transmission and reception of data packets. While BER represents the number of data bits received in error with respect to the total number of bits transmitted, the PER is obtained by finding the number of packets in error with respect to the total number of packets transmitted. We consider a packet in error if any error in the 802.11a OFDM SIGNAL symbol occurs or a CRC failure occurs in 802.11b since the packet then cannot be recovered. While the BERs provide insights into the fundamental interactions at the bit level, the PERs are useful practically for understanding the effects at higher layers.

B. BER versus E_b/N_0

Fig. 1 shows the BER performance versus E_b/N_0 for a representative sample of the many data modes and rates which were studied [17]. In each subplot, one curve shows the performance of 802.11b without a RAKE receiver architecture—the performance is very poor. With a RAKE receiver, however, 802.11b sometimes performs as well or better than 802.11a although with lower data rates. In the case of 802.11a, the 12 Mbps data rate is robust and provides several dBs advantage over higher rates. However, it is also to be noted that lower rates need to transmit longer than higher rate modes in order to send the same amount of information. We also see that the curves tend to flatten at the higher SNR region as the performance becomes more dominated by the delay spreads. Although the rms delay spread is within 0.8 μs for the cases studied in these figures, there are still multipaths beyond 0.8 μs producing adjacent symbol interference. In the case of 802.11b without RAKE receiver, multipath is the dominating factor since even at high SNRs, BERs are never better than 2%. We observe in some cases, that higher data rates sometimes provide better BER performance due to different modulation formats employed. At all five sites, one observes a crossover of the curves for the 802.11a 12 Mbps and the RAKE-enabled 802.11b 11 Mbps modes (fairest means of comparing the DSSS and OFDM architectures). The 802.11b performance is better for very low SNR, while 802.11a is better with higher received power.

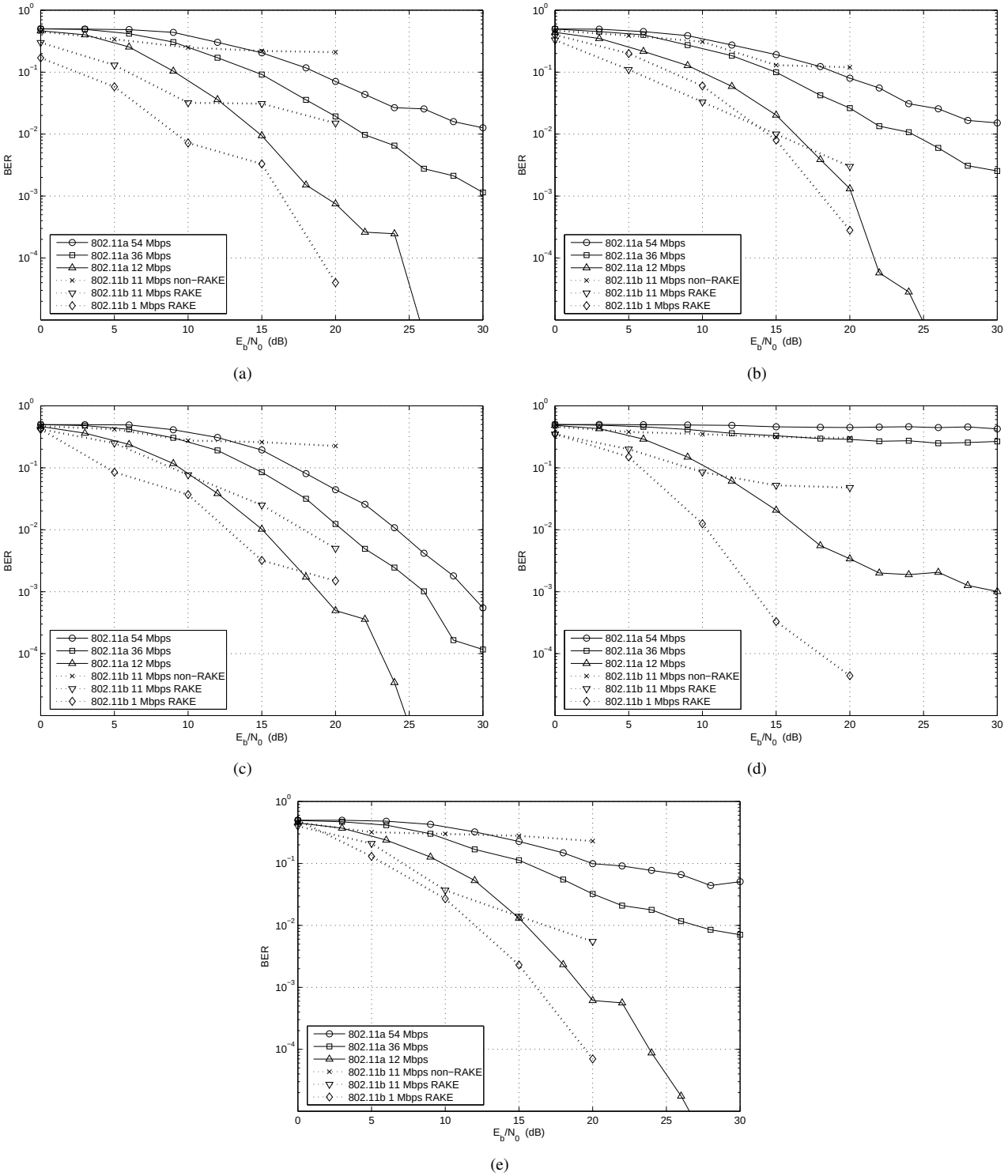

Fig. 1. BER versus SNR for 802.11a and b (100 m distance and 1.5 m antenna heights) at (a) Gusev1 Site1, (b) Gusev1 Site2, (c) Gusev1 Site3, (d) Hematite4, and (e) Hematite5.

C. PER versus Distance

Table IV shows PER versus transmission distance assuming 1 W radiated power and 1.5 m antenna heights. Both 802.11a and b perform well, in general, for a receiver within several hundred meters from the transmitter although 802.11a is clearly superior. When the distance between transmitter and receiver is 500 m or less, dependence of PER upon distance is weak, and overwhelmed by favorable or unfavorable terrain features and multipath peculiarities of a given transmitter/receiver location pair. We do not doubt, of course, that error rate does increase with transmission distance. We simply observe that in an environment such as the Martian surface, the terrain features play the dominant role. Finally, we note that results with very low PER values must be used with caution as they are not statistically significant due to the small number of packet errors observed from transmitting 20,000 data packets.

TABLE IV
PER VERSUS DISTANCE (1.5 M ANTENNA HEIGHTS; 1 W RADIATED POWER). ZERO PACKET ERRORS IN 20,000 PACKETS ARE DENOTED WITH '—'.

dist (m)	Gusev1 Site1		Gusev1 Site2		Gusev1 Site3		Hematite4		Hematite5	
	802.11a	802.11b	802.11a	802.11b	802.11a	802.11b	802.11a	802.11b	802.11a	802.11b
20	0.0008	0.0983	0.0003	0.1145	0.0002	0.1000	0.0262	0.2113	0.0037	0.1280
50	0.0004	0.0768	0.0004	0.0823	—	0.0273	0.0272	0.2619	0.0012	0.0950
100	0.0001	0.0572	0.0001	0.0323	—	0.0159	0.0138	0.1667	0.0004	0.0724
200	0.0001	0.0281	0.099	0.5050	0.0001	0.0297	0.0026	0.1196	0.0001	0.0354
500	—	0.0158	0.067	0.5313	1.0	0.5417	0.0001	0.0478	0.0004	0.0370
1000	1.0	0.9619	N/A	N/A	1.0	1.0	0.4405	0.3312	1.0	1.0

D. Effects of Antenna Height

Higher antenna heights can affect the performance of any communication system by improving line-of-sight and thus increasing received power. However, they can also result in higher delay spreads resulting in decreased performance at the receiver. Furthermore, there are obvious physical limitations in antenna height in rover and sensor applications. Simulations of BER versus antenna height (transmitter and receiver antenna heights varied together) were done for the different sites using 100 μW radiated power so that any gains from antenna height would be more apparent. Results for 802.11a are given in Fig. 2(a) and show significant improvements with increased antenna heights due to more received power which, as will be seen in subsection III-E, can be critical for 802.11a. In addition, increased delay spread due to increased antenna height is still well within the guard interval of 802.11a allowing good performance. Results for 802.11b with a RAKE receiver are given in Fig. 2(b) and do not show significant improvements with increasing antenna heights. This may be because the benefit due to more received power is nearly cancelled by the loss due to increased delay spreads.

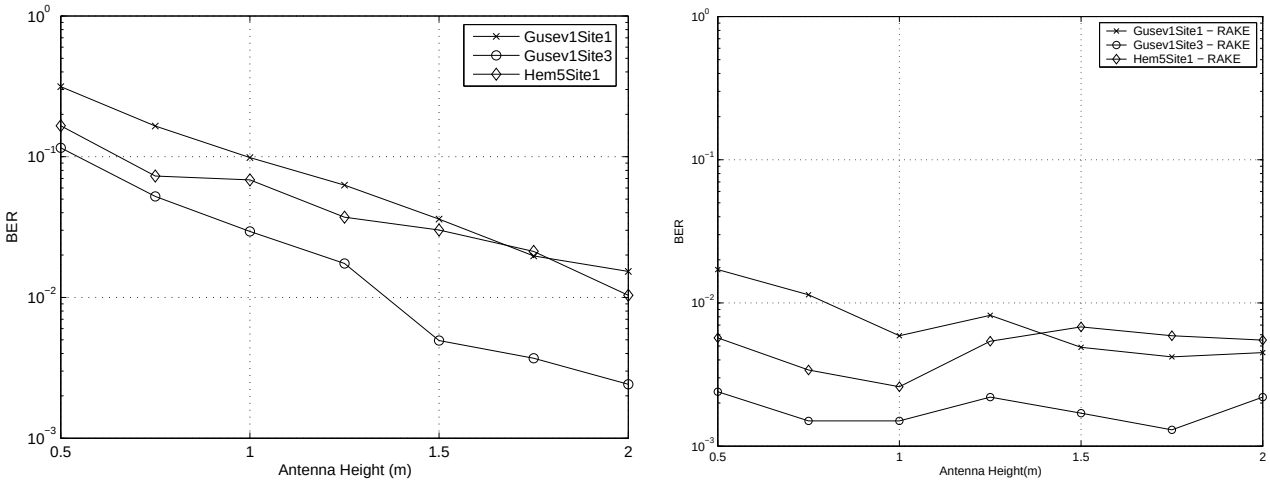

(a) (b)

Fig. 2. BER vs. antenna height for (a) 802.11a and (b) 802.11b using RAKE receiver (100 μW radiated power).

E. Effects of Radiated Power

It is important to study the effects with different radiated powers since an actual planetary exploration device would likely adjust its transmitter power dynamically, to achieve acceptable performance with the least possible power consumption. As an example of our results, consider Gusev1 Site1 with a transmitter/receiver distance of 100 m and 1.5 m antenna heights. For

802.11a we have found that below about 10 mW of radiated power the receiver is in a power-limited region. In this region, when the radiated power is 1 μW the PER is found to be 0.985. An increase in radiated power to 10 μW, 100 μW, 1 mW and 10 mW leads to a decrease in PER values to 0.381, 0.0225, 0.0021 and 4×10^{-4} respectively. However, a further increase in radiated power to 100 mW and 1 W results in a PER of 2.5×10^{-4}, and 2.0^{-4} respectively, a marginal improvement over the 10 mW case. Similarly, for 802.11b without a RAKE structure the power-limited region is up to about 1 mW when a PER of 0.0625 is obtained. An increase in radiated power to 1 W provides a PER of 0.0516, a marginal improvement over the 1 mW case.

The existence of the power-limited region can be explained by considering the multipath environment. For the Gusev1 Site1 location, the rms delay spread at 5 GHz is 0.105 μs which is much less than the 0.8 μs guard period of 802.11a. Thus, 802.11a can handle this multipath environment quite well and its performance keeps improving with the radiated power. As the radiated power becomes large and noise is no longer the dominating factor, multipaths with delays exceeding 0.8 μs now become the dominating factor and begin affecting performance due to adjacent symbol interference thus limiting further performance improvements. Similarly, in the case of 802.11b when the multipath-dominated region is reached, the effect of inter-symbol interference rather than the transmit power plays the critical role. Our study also provides an approach to finding the power-limited and the multipath-limited regions for any given transmitter/receiver location pair. This can be very effective in planning rover paths which can minimize communication system power consumption.

IV. Conclusions

We have investigated the applicability of 802.11a and b WLAN standards for proximity networks on the Martian surface. By utilizing high-resolution DEMs of the Martian surface, we have presented a methodology to incorporate multipath effects between a transmitter and receiver into a WLAN simulation. We have observed that successful communication as measured by BERs and PERs is possible within a few hundred meters of the transmit antenna for both standards when the rms delay spread is not too severe, radiated power is a few tens of milliwatts, antenna heights are about 1.5 m above ground, and a RAKE receiver is used in 802.11b. With sufficient received power, however, 802.11a has superior PHY performance as compared to 802.11b since the former is less affected by multipaths. Our work suggests that proximity networks based on commercial WLAN standards and in particular, 802.11a could be effectively utilized on the Martian surface.

Acknowledgment

Support of this research was through NASA Glenn Research Center, Grant #NAG 3-2864.

References

[1] A. Doufexi, S. Armour, B. Lee, and D. Bull, "An evaluation of the performance of IEEE 802.11a and 802.11g wireless local area networks in a corporate office environment," in *Proc. IEEE ICC*, vol. 2, Anchorage, AK, May 2003, pp. 1196–1200.

[2] X. Zhao, J. Kivinen, P. Vainikainen, and K. Skog, "Propagation characteristics for wideband outdoor mobile communications at 5.3 GHz," *IEEE J. Select. Areas Commun.*, vol. 20, no. 3, pp. 507–514, Apr. 2002.

[3] Z. Wang, E. K. Tameh, and A. R. Nix, "Statistical peer-to-peer channel models for outdoor urban environments at 2 GHz and 5 GHz," in *Proc. IEEE VTC*, vol. 7, Los Angeles, CA, Sep 2004, pp. 5101–5105.

[4] M. V. Clark, K. K. Leung, B. McNair, and Z. Kostic, "Outdoor IEEE 802.11 cellular networks: Radio link performance," in *Proc. IEEE ICC*, New York, NY, 2002.

[5] I. Bradaric, R. Dattani, A. P. Petropulu, F. L. Schurgot, and J. Inserra, "Analysis of physical layer performance of IEEE 802.11a in an ad-hoc network environment," in *Proc. IEEE MILCOM*, vol. 2, New Orleans, Oct 2003, pp. 1231–1236.

[6] T. Rappaport, *Wireless Communications Principles and Practice*, 2nd ed. New Delhi: Pearson Education, 2002, chap. 4,5.

[7] ATDI, Feb 2007, <http://www.atdi.com/icstelecom.php>.

[8] V. Chukkala, P. D. Leon, S. Horan, and V. Velusamy, "Modeling the radio frequency environment of Mars for future wireless, networked rovers and sensor webs," in *Proc. IEEE Aerospace Conf.*, Big Sky, MT, 2004.

[9] F. Anderson, A. Haldemann, N. Bridges, M. Golombek, and T. Parker, "Analysis of MOLA data for the Mars exploration rover landing sites," *J. Geophys. Res.*, vol. 108, no. E12, Dec. 2003.

[10] R. Kirk, E. Howington-Kraus, B. Redding, D. Galuszka, T. Hare, B. Archinal, L. Soderblom, and J. Barrett, "High-resolution topomapping of candidate MER landing sites with Mars orbiter camera narrow-angle images," *J. Geophys. Res.*, vol. 108, no. E12, Dec. 2003.

[11] USGS, http://webgis.wr.usgs.gov/mer/moc_na_topography.htm, June 2006.

[12] G. Hufford, A. Longley, and W. Kissick, "A guide to the use of the ITS irregular terrain model in the area prediction mode," *NTIA Report No. 82-100*, Apr. 1982.

[13] S. Cummer and W. Farrell, "Radio atmospheric propagation on Mars and potential remote sensing applications," *J. Geophysical Research*, pp. 104,14,149–14,157, Jun. 1999.

[14] C. Ho, S. Slobin, M. Sue, and E. Njoku, "Mars background noise temperatures received by spacecraft antennas," *The Interplanetary Network Progress Report*, vol. 42-149, May 2002.

[15] D. Hansen, M. Sue, C. Ho, M. Connally, T. Peng, R. Cesarone, and W. Horne, "Frequency bands for Mars in-situ communications," in *Proc. IEEE Aerospace Conf.*, Big Sky, MT, 2001.

[16] *IEEE Part 11: wireless LAN medium access control (MAC) and physical layer (PHY) specifications: High-speed physical layer in the 5 GHz, IEEE Std. 802.11a-1999, Sept 1999*, IEEE Std. 802.11a, 1999.

[17] D. Borah, A. Daga, G. Lovelace, and P. DeLeon, "Performance evaluation of the IEEE 802.11a and b WLAN physical layer on the Martian surface," in *Proc. IEEE Aerospace Conference*, Big Sky, MT, Mar. 2005.

[18] B. Pearson, "A review of spread spectrum techniques for ISM band systems," *Intersil Corp, App Note 9820*, Oct 1998.

[19] A. Doufexi, S. Armour, P. Karlsson, A. Nix, and D. Bull, "A comparison of HIPERLAN/2 and IEEE 802.11a," *IEEE Commun. Mag.*, May 2002.